FAST-ION STOPPING POWER IN HOT, DENSE, STRONGLY-COUPLED PLASMA

B. Crowley

JOURNAL DE PHYSIQUE
Colloque C7, supplément au n°12, Tome 49, décembre 1988

FAST-ION STOPPING POWER IN HOT, DENSE, STRONGLY-COUPLED PLASMA

B.J.B. CROWLEY

Atomic Weapons Establishment, Aldermaston, GB-Reading RG7 4PR, Great-Britain

Résumé - L'expression relativiste de la formule de Bethe pour le ralentissement de particules rapides (fonction diélectrique transverse) dans les plasmas denses et fortement corrélés ($\Gamma_{ocp} >> 1$) est établie. Un modèle d'atome moyen adaptable sur PC est décrit. Il donne accès aux contributions lié-libre et libre-libre de la fonction d'excitation plasma, lesquelles améliorent les modèles OCP ou Debye-Hückel. Dans les plasmas fortement ionisés ($Z^* >> 1$), il arrive fréquement que les ions soient fortement couplés, alors que les électrons libres ne le soient que faiblement. Ainsi, bien que le traitement DH demeure valable pour les électrons, l'approximation OCP pour la composante ionique peut ne pas être valable à toutes densités. Le modèle décrit tient compte de la polarisation électronique à l'intérieur de la sphère ionique, ainsi que l'influence de l'écrantage électronique sur la dynamique des ions. Ces effets sont incorporés dans l'abaissement du continu, lequel inclue les fluctuations du microchamp électrique. Le modèle de plasma donne un traitement raisonnable des effets collectifs au voisinage de la résonance. Puisque la précision spectroscopique n'est pas requise dans les calculs de pouvoir d'arrêt, si l'on satisfait aux règles de somme, on utilise une formule analytique approchée pour les niveaux atomiques. On omet les transitions lié-lié, la force d'oscillateur correspondante étant approximativement transférée aux transitions lié-libre. On calcule les fonctions d'excitation et les pouvoirs d'arrêt pour Al à 100 eV et Pb à 300 eV avec des densités de plasma usuelles.

Abstract - The relativistic form of the Bethe fast-ion stopping power involving the transverse dielectric function, as given by Landau and Lifshitz, is applied to calculation of atomic ion stopping in hot, dense plasmas in which the ions are strongly coupled ($\Gamma_{ocp} >> 1$). An average-atom plasma model, suitable for implementation on a PC spreadsheet, is described. This model, which provides the basis of a calculation of a bound-free and free-free representation of the plasma excitation function, incorporates several novel enhancements over the standard one-component plasma (OCP) or Debye-Hückel models. In highly ionised ($Z^* >> 1$) plasmas, a frequently found situation is that the ions appear strongly coupled while the continuum electrons remain weakly coupled. Thus, while the Debye-Hückel treatment may therefore remain valid for the electrons, the OCP approximation for the ion component may not hold except at very much higher densities. The model therefore allows for electron polarisation within an ion sphere and treats the influence of electron screening on the ion dynamics. These effects are incorporated into a continuum lowering model which includes microfield (Stark) fluctuations. The plasma model also provides a reasonable treatment of the plasma collective effects around the plasma "resonance". Since spectroscopic accuracy is not demanded for stopping power calculations provided that the appropriate sum rule is obeyed, use is made of an approximate analytical formula for the atomic energy levels. Bound-bound transitions are omitted - the bound-bound oscillator strength being appropriately transferred to the bound-free. Calculations of excitation functions and stopping powers are presented for 100eV aluminium and 300eV lead plasmas at normal densities.

1 - INTRODUCTION

Rapid progress in desktop computing power in recent years now makes it possible to perform quite detailed and sophisticated calculations of plasma models with quite modest resources. Moreover, the application of specialised software, rather than the more familiar general programming languages, like FORTRAN, can permit the rapid development of complex numerical models within a flexible framework. This work describes the application of such a tool, the scientific spreadsheet, to the study of hot, dense, LTE plasma under possible ICF conditions. Spreadsheets are ideal for developing and implementing analytical and semi-analytical models especially in "what if?" and "try-it-and-see" contexts. Flexibility comes particularly from the cyclic nature of the calculation which enables new ideas to be plugged in almost anywhere and have access to every parameter. The user has complete control over the whole calculation which can be viewed through a selected window as it is running, and can readily redefine any part of it. Input data may consist of formulae, rather than numbers, and can even reference the calculation. The complexity of the user interface does however give rise to problems of documentation!

For its theme, this paper considers the calculation of fast heavy-ion stopping in hot, dense LTE plasma (dense in the sense that the plasma is strongly coupled; hot in the sense that the plasma is Lorentzian and non-cohesive ($P > 0$), and not highly degenerate) using the Landau-Lifshitz form of the stopping power [1] for fast heavy-ions, namely,

$$\frac{dE}{dx} = - \left[\frac{Z_{eff}\,\Omega}{\beta} \right]^2 \frac{\alpha}{\hbar c} L_s \qquad (1)$$

with

$$L_s = \ln\left[\frac{2mc^2}{\bar{I}} \right] + 2\ln(\beta\gamma) - \beta^2 \qquad (2)$$

where $\bar{I}$ is the usual mean energy loss per collision, $\beta = v/c$, $\gamma = (1 - \beta^2)^{-\frac{1}{2}}$, v is the ion velocity, and $E = (\gamma - 1)Mc^2$ is the ion energy. Other symbols appearing are as follows: α denotes the fine-structure constant; M the ion mass; m the electron mass; Z_{eff} the ion *effective charge*; and the limiting plasma frequency is $\Omega = (Z/Z^*)^{\frac{1}{2}}\,\omega_e \equiv \hbar c(4\pi\alpha\hbar c Z n_i/mc^2)^{\frac{1}{2}}$, where n_i is the plasma-ion (number) density, Z is the atomic number of the plasma, and Z^* is the mean ionisation of the plasma. The mean energy loss $\bar{I}$ is the logarithimic average weighted by the plasma *excitation function*, $\Pi(\omega)$ which is given in terms of the plasma dielectric function $\epsilon(\omega)$ by

$$\Pi(\omega) = - \frac{2\omega}{\pi\Omega^2} \mathrm{Im}\left[\frac{1}{\epsilon(\omega)} \right] \qquad (3)$$

ie,

$$\ln(\bar{I}) = \int_0^\infty \ln(\omega)\,\Pi(\omega)\,d\omega\,, \qquad \int_0^\infty \Pi(\omega)\,d\omega = 1. \qquad (4,5)$$

the normalisation property being an expression of the Bethe f-sum rule. In taking these integrals to infinity, one is ignoring the possibility of *inner shell corrections* due to there being an upper limit to the energy loss in a single collision, and that this energy must be at least sufficient to cause ionization. Moreover equation (1) is valid in an impulse approximation which neglects motion of the plasma electron before the collision. It is failure to take proper account of these effects that leads to a stopping power that is too small or even negative for low ion energies. This is due to an excessive *negative* contribution, in equation (1), from the most tightly bound electrons. An effective palliative is therefore to extend the integration over ω only as far as $q \equiv 2M^2mc^2(\gamma^2-1)/(M^2+2\gamma Mm+m^2)$ which is the maximum energy that can be lost in an elastic collision with a stationary free electron. This both limits the maximum energy loss in a single collision and removes contribution from electrons that are too tightly bound to be ionized. As a result the validity of equation (1) is enhanced in the sense that the implicit approximations are *less bad* near the end of the particle range. Indeed, with these corrections, L_s generally does not become negative. Calculations of the proton stopping power in the MeV range confirm that the stopping power calculated using (1) *increases* when the contribution from inaccessible inner-shells is removed. The corrections are applied by replacing L_s in (1) by L_s' where

$$L_s' = L_s \int_0^q \Pi(\omega)\,d\omega - \int_0^q \ln\left[\frac{\omega}{\bar{I}}\right]\Pi(\omega)\,d\omega \qquad (6)$$

in which L_s continues to be given by (2).

A plasma model yielding the plasma dielectric function is therefore a means of calculating the stopping power. The model, which is described in the following, incorporates several novel features and is suitable for implementation on a spreadsheet.

2 - THE PLASMA MODEL

2.1 - Electronic properties and calculation of the dielectric function.

The plasma dielectric function $\epsilon(\omega)$ is calculated in terms of the plasma properties including the *reduced opacity* [2] $\kappa(\omega)$, and the bound electron *optical activity* $f(\omega)$, according to

$$\epsilon = \epsilon' + i\epsilon'' \tag{7}$$

$$\epsilon'(\omega) = 1 - \omega_e^2\left[\frac{1}{\omega^2 + \nu^2} + \frac{f(\omega)}{Z^*\omega^2}\right], \qquad \epsilon''(\omega) = \hbar c\rho\kappa(\omega)/\omega \tag{8,9}$$

The function $f(\omega)$ vanishes at very low frequencies well below the photoionization threshold, and tends to $Z - Z^*$, the average number of bound electrons, in the limit of $\omega \to \infty$.

The reduced opacity, $\kappa = \kappa_f + \kappa_b$, separates into a part $\kappa_f(\omega)$ due to continuum (free) electrons (free-free processes) and a part $\kappa_b(\omega)$ due to bound electrons. The free-free part, κ_f is calculated as

$$\rho\kappa_f(\omega) = \frac{\nu^2\omega_e^2 T\,(1 - \exp(-\omega/T))}{\nu_c\hbar c\omega\,(\omega^2 + \nu^2)} + n_i Z\sigma_T \tag{10}$$

in which the first term is a universal form of the continuum-electron absorption opacity, while the second describes Thomson scattering and is only important at high frequencies. Here, σ_T is the Thomson cross-section. The collision frequency ν appearing in equations (8-10) is expressed in terms of the conductivity collision frequency,

$$\nu_c = \frac{\sqrt{2\pi}}{32}\,\frac{Q_e^2}{\gamma_e Z^*}\,\omega_e\Lambda_e \ln(\Lambda_C) \tag{11}$$

(in which γ_e is the Spitzer correction [3] for electron - electron collisions) and the Kramers bremsstrahlung collision frequency,

$$\nu_b = \frac{\sqrt{2\pi}}{3\sqrt{3}}\,\frac{Q_e^2}{Z^*}\,\omega_e\Lambda_e \tag{12}$$

by

$$\nu^2 = g_{ff}\nu_b\nu_c \Big/ \left[1 + \frac{\Delta_f}{\left[1 + (\omega/\omega_e)^2\right]^2}\right] \tag{13}$$

in which are introduced the *Gaunt factor* [4], g_{ff}; the electron-electron coupling parameter $\Lambda_e = \ell/D_e$; and the effective charge Q_e for close electron-ion collisions (for Lorentzian collisions, $Q_e \simeq Z^*$); and the *Coulomb logarithm*, $\ln(\Lambda_C)$. The electron *Landau length* ℓ and the electron *Debye length* D_e, are calculated according to the "exact" expressions [5],

$$\ell = \alpha\hbar c \Big/ \frac{\partial\mu}{\partial\ln(n_e')}, \qquad D_e = \frac{\hbar c}{\omega_e}\left[\frac{1}{mc^2}\,\frac{\partial\mu}{\partial\ln(n_e')}\right]^{\frac{1}{2}} \tag{14,15}$$

which involve the *chemical potential* $\mu(n_e', T)$ for a free-electron gas of density n_e' and temperature T. These equations relate D_e and ℓ to the electron density fluctuations and allow for correlations due to degeneracy. The effective thermal energy, $\theta = \partial\mu/\partial\ln(n_e)$, is the "transport energy" ($n_e\theta$ is the electronic bulk modulus) and is equal to $T\,\langle\Delta N_e^2\rangle/\langle N_e\rangle$ where ΔN_e is the fluctuation in the number N_e of electrons in a fixed volume V. In addition, the *polarisation* of the electron density in the vicinity of a strong ion field ($Z^* >> 1$) is treated by virtue of the chemical potential being correctly expressed in terms of $n_e' = Z_2^* n_i$ which is the electron density *at the surface of the ion-sphere* [6], instead of the average density, $n_e = Z^* n_i$. An analytical estimate of the ratio Z_2^*/Z^* is found to be

$$(1 + X + X^2/2 + X^3/6)\exp(-X)$$

where $X = R/D_e$ and R is the ion-sphere radius. This formula results from assuming a polarisation potential of the form

$$V_p(r) \equiv V_p(xD_e) = (Z^*/D_e)(ax^2 + bx + (\exp(-x) - 1)/x)$$

and determining the coefficients a and b from the conditions $\partial\rho_e/\partial r = 0$ at $r = R$; and $4\pi\int_0^\infty \rho_e r^2 dr = -Z^*$,

with the electron charge density $\rho_e(r)$ given by Poisson's equation, $4\pi\rho_e(r) = -\nabla^2 V_p$. Note also that whereas the ionic component of the plasma may be strongly coupled, the electronic component is assumed to be weakly coupled. This prescription provides an analytic estimate of the Thomas–Fermi chemical potential for given Z^*. The same model is used to provide the electron polarisation correction to the large–Γ limit of (29).

The Coulomb logarithm is given by a minor generalisation of the RPA form [8], ie,

$$\ln(\Lambda_C) = \frac{1}{2}\left[p\ln[1 + \Lambda_D^2(Z^*+q)] + q\ln[1 + \Lambda_D^2(Z^*-p)\ ] - 1\ \right] \qquad (16)$$

where p is the fractional part of Z^* and $p + q = 1$. For the logarithm argument, $\Lambda_D(z)$, the following formula, which interpolates between the classical and quantal limits, is used

$$\Lambda_D(z) = \frac{3}{z\Lambda_e}\left[\ 1 - \exp(-2z\eta/\sqrt{3})\ \right] \qquad (17)$$

where $\eta = \alpha\hbar c/\omega_e D_e$ is the Sommerfeld parameter for a Coulomb collision between an electron with velocity $\omega_e D_e$ and an ion of unit charge. The classical and quantal limits are respectively $\eta z >> 1$ and $\eta z << 1$.

The formula (10) for κ_f is valid at low frequencies ($\omega << \omega_e$, when it yields the classical conductivity and skin–depth formulae) and at high frequencies when it yields the Kramers inverse–bremsstrahlung formula with a Gaunt factor [4,10,11]. The correspondence with the formalism of Landau and Lifshitz [9] is made by identifying $\pi g_{ff}/(\sqrt{3}(1+\Delta_f))$ and $\pi g_{ff}/\sqrt{3}$ respectively with the low frequency ($\nu << \omega << \omega_e$) and high frequency Coulomb logarithms. In practice, the quantity Δ_f is best determined by enforcing the sum rule.

The contribution of the bound electrons to the opacity is taken as being given by

$$\rho\kappa_b(\omega) = \frac{\pi F\ \omega_e^2\ (1 - \exp(-\omega/T))}{Z^*\hbar c\ \omega\ (\omega^2 + \Gamma^2)} \qquad (18)$$

where $\Gamma(\omega)$ is taken to be the impact width of a level bound by ω (this is an unimportant correction, and is applied only to remove possible divergence at $\omega = 0$) and F is provided by the atomic model as described in section 3.

2.2 – Ion dynamics and microfield fluctuations.

In dense strongly coupled plasmas, the atomic states are strongly influenced by the plasma microfield which can be represented as a static (average) plasma polarisation part ΔV_p, and a fluctuating part ΔV_{fl}. The total continuum lowering used in the determination of the ionization state is taken as $\Delta V_{cl} = \Delta V_p + \Delta V_{fl}$ which accounts for the ionisation of upper levels of an atom due to fluctuations in the local microfield. The plasma polarisation ΔV_p is normally dominated by the electron–electron and electron–ion interactions (eg. see [6]). However, in a plasma in which the usual OCP approximation fails, but in which the ion–ion interaction can be reasonably treated in the Debye–Hückel approximation through the plasma Debye length $D = (1/D_e^2 + 1/D_i^2)^{-\frac{1}{2}}$, there is apparently an additional contribution to the continuum lowering due to the effect of electron screening on the ion–ion electrostatic free energy. For $Z^* >> 1$ this amounts to

$$3\,\frac{D^2 Z^* \alpha\hbar c}{R^3}\left[\ 1 - \frac{D^2}{2D_e^2} - \frac{D^2}{D_i^2}\ \right] \qquad (19)$$

which vanishes in the OCP limit when $D_e \to \infty$, $D \to D_i$. In both weakly and very strongly coupled plasmas, this contribution is typically very small (often less than the uncertainty in the electronic contribution). In the latter case, the formula may lack some validity. However, in moderately strongly–coupled plasmas, the concept of an ion Debye length may continue to have some validity if electron screening sufficiently weakens the ion–ion coupling. In such cases, a small, but significant, contribution can arise from this term.

The treatment of the ion dynamics assumes that the ions interact through a nearest–neighbour potential of the form,

$$V_{12} = \alpha\hbar c\,\frac{Z_1\ Z_2}{r_{12}}\exp(-r_{12}/d_{12}) \qquad (20)$$

where d_{12} is a dynamical screening length due to screening by the continuum electrons (bound electrons too if the collisions are non–Lorentzian). If $Z_1 << Z_2$ (or *vice–versa*) then $d_{12} \sim D_e$, otherwise the additional electron polarization in the dipolar ion field gives rise to $d_{12} < D_e$. These, together with the requirements of Thomas–Fermi scaling [6] and consistency with the form of the Lindhard potential [16,7] which describes screening by *bound* electrons, suggests the following form for d_{12}

$$d_{12} = \frac{\left[Z_1^{4/3} + Z_2^{4/3}\right]^{1/2}}{\left[Z_1^{2/3} + Z_2^{2/3}\right]} D_e \qquad (21)$$

In particular, when $Z_1 = Z_2$, $d_{12} = d = D_e/\sqrt{2}$. The effect of this screening on the ion-ion coupling may be represented by an *effective ion-ion Landau length, L* defined to be the distance of closest approach for a thermal ion with energy T_i where T_i is the ion temperature. The definition is the same as the usual one except that the potential is (20) rather than Coulombic and the thermal kinetic energy is ascribed at the effective lattice distance r_0, which is the mean ion-ion separation in the zero-T configuration (represented in terms of randomly packed hard spheres) rather than at infinite separation. In this way one can treat both the effect of close packing at high density, and the effect of electron screening. This definition yields L according to

$$L = d\lambda \qquad (22)$$

$$\lambda = \lambda_0 e^{-\lambda} \qquad (23)$$

$$\lambda_0 = \left[\frac{d}{L_{ocp}} + \frac{d}{r_0} e^{-r_0/d} \right]^{-1} \qquad (24)$$

where L_{ocp} is the OCP Landau length ($d \sim \infty$, $r_0 \sim \infty$). The ratio L/L_{ocp} expresses the weakening of the ion-ion coupling by electron screening and polarisation. We can regard this as being equivalent to a reduction in the effective ion charge and apply the appropriate modifications to the ion plasma frequency, Ω_i and Debye length D_i in accordance with

$$\Omega_i = \Omega_i^{ocp} \left[\frac{L}{L_{ocp}} \right]^{\frac{1}{2}} \qquad D_i = D_i^{ocp} \left[\frac{L_{ocp}}{L} \right]^{\frac{1}{2}} \qquad (25,26)$$

where X^{ocp} or X_{ocp} denotes the value of X in the standard OCP model.

In considering the continuum lowering due to polarization of such a plasma, it is found to be convenient to represent the interaction of an ion with the surrounding plasma in terms of an *effective perturber charge,* Q_i where

$$Q_i = \frac{T_i}{4\pi\alpha\hbar c D^2 n_e} \qquad (27)$$

where D is the plasma Debye length as given by $D = (1/D_e^2 + 1/D_i^2)^{-\frac{1}{2}}$. The concept of an effective perturber charge is particularly useful for describing continuum lowering in plasmas containing more than one ion species (the many-component plasma) especially those consisting of components of widely differing Z. For the OCP, $Q_i = Z^*$. In terms of Q_i, the effective plasma coupling parameter is

$$\Gamma = \frac{Q_i}{Z^*} \Gamma_{ocp} \equiv \frac{Q_i L_{ocp}}{Z^* R} \qquad (28)$$

where Γ_{ocp} is the OCP coupling parameter [12]. (In a many-component plasma, Γ is defined for each ion species.)

In terms of these parameters, the continuum lowering is given by a suitably modified form of the Stewart-Pyatt formula [6,17],

$$\Delta V_p = \frac{T_i}{2Q_i} \left[\left(1 + \frac{R}{3D_e}\right) \exp\left[-\frac{R}{D_e}\right] + \frac{2R}{3D_e} \right] \left[1 - \left[(3\Gamma)^{3/2} + 1 \right]^{2/3} \right] \qquad (29)$$

which allows for polarization of the electrons within the ion sphere even when the ions are strongly coupled ($\Gamma >> 1$), ie, the formula allows for the possibility that $\Gamma >> 1$ at the same time as $D_e \lesssim R$. If $\Gamma > 4.96045$ an extra term equal to $3.266\Gamma^{\frac{1}{4}} - 0.57844\Gamma - 2.0048$ is added within the second parenthesised factor in order to yield the correct high-density limit [6,13]. In the weak coupling limit, the formula is indistinguishable from the "standard" plasma polarisation result of Debye-Hückel theory.

The fluctuation component of the continuum lowering is taken to be the rms nearest-neighbour potential, seen by a small test charge at the mid barrier, less the same potential due to the perturber when at the lattice distance r_0. This gives, approximately

$$\Delta V_{fl} \simeq -2Z^*\alpha\hbar c \left[\frac{e^{-r_1/2D_e}}{r_1} - \frac{e^{-r_0/2D_e}}{r_0} \right] \qquad (30)$$

where $r_1 = R/\langle\beta\rangle^{\frac{1}{2}}$ and $\beta = (R/r)^2$ (which is the microfield, in the absence of screening, in units of the normal field, $- Z^*\alpha\hbar c/R^2$). The average $\langle\beta\rangle$ is calculated using a nearest-neighbour distribution corrected for Coulomb repulsion at close distances, ie,

$$\langle\beta\rangle \simeq \frac{\int_0^\infty \beta P(\beta)\, \exp\left[-2\beta^{\frac{1}{2}} L/R \right] d\beta}{\int_0^\infty P(\beta)\, \exp\left[-2\beta^{\frac{1}{2}} L/R \right] d\beta} \tag{31}$$

in which L is the effective Landau length, and $P(\beta)d\beta$ is the Poissonian nearest-neighbour distribution, $P(\beta) \propto \beta^{-5/2} \exp(-\beta^{-3/2})$. A saddle point approach is used to estimate the ratio of the integrals with an analytic formula when L/R is not too small.

Although somewhat crudely implemented, this method does seem to account for the gross effects and yields reasonable edge widths that are in agreement with the scarce amount of available experimental data [15]. The same approach is used to estimate the mean square electric field to determine the Stark widths of bound levels. With $r_2 = R/\langle\beta^2\rangle^{\frac{1}{4}}$, the rms electric field due to the nearest perturber is estimated by

$$\langle E^2\rangle^{\frac{1}{2}} \simeq Z^*\alpha\hbar c \left[\frac{e^{-r_2/D_e}}{r_2^2} + \frac{e^{-r_1/D_e}}{r_1 D_e} \right] \tag{32}$$

3 - ATOMIC PHYSICS MODEL

A model of the bound electronic states within the atomic ions is required in order to determine the three quantities Z^*, F, and f that feature in the above plasma model. The model used is a simplified version of the average-atom in which the bound electron energies are estimated by an analytical formula. (This is not a necessary approximation and indeed, for realistic calculations, is generally inadvisable. The spreadsheet does however allow the replacement of such estimates by more accurately known values.) The average-atom prescription is as follows. Given a set of energy levels ϵ_n, which may depend on the value of Z^*, the average-atom level populations, N_n , and the average ionization Z^* are determined *self-consistently* from the following equations,

$$N_n = \frac{w_n}{1 - \exp(-(\mu+\epsilon_n)/T)} \quad , \qquad Z^* = Z - \sum_n N_n \tag{33,34}$$

where w_n is the statistical weight of the level; together with the constitutive relations for the ionization energies, ϵ_n and the chemical potential, μ. The ionization energies are calculated as described below, while, for the chemical potential, an analytical parameterisation based on the work of Latter [14] is used. The required functions $F(\omega)$ and $f(\omega)$ are then given as follows

$$F(\omega) = \sum_n N_n \epsilon_n^2 \exp\left[-\tfrac{1}{2} t_n^2\right] + \sum_n N_n \epsilon_n^2 \tag{35}$$

$(t_n < 0,\ \omega > 7\lambda_n^2/\epsilon_n)$ $\qquad$ $(t_n > 0)$

$$f(\omega) = \sum_n N_n \left[1 + \frac{1}{2}\left[\frac{\epsilon_n}{\omega} (1+\lambda_n^2) \right]^2 \ln\left\{ \left[1 - \left[\frac{\omega}{\epsilon_n}\right]^2 - 2\lambda_n^2 \right]^2 + 4\lambda_n^2 \left[1-\lambda_n^2\right] \right\} \right] \tag{36}$$

where

$$t_n = \frac{1}{\lambda_n} \left[\frac{\omega}{\epsilon_n} - 1\right] \left[2 - \frac{\pi}{2}\right]^{\frac{1}{2}} - \left[\frac{\pi}{2} \right]^{\frac{1}{2}} \tag{37}$$

and λ_n is the ionization edge "width", expressed as the rms deviation, divided by the ionization energy ϵ_n at the average position. Since the ionization energies, ϵ_n are given only on the gross energy scale of the hydrogenic principal quantum number, n, the edge broadening model should take account of inhomogeneous broadening due to spin-orbit and configurational splitting, as well as homogeneous broadening caused by, in particular, Stark and Doppler broadening of the bound level, and fluctuations in the continuum threshold. The last process is by far the dominant source of homogeneous edge broadening.

The above formula for F describes a quasi-Gaussian-broadened edge profile, while the optical

activity $f(\omega)$ derives from the analytic form of the Kramers–Krönig transform of broadened $1/\omega^3$ ionization profile. The latter is insensitive to the precise form of the edge broadening profile. Scaling factor(s) may be applied to F to ensure accurate compliance with the sum–rule.

The following describes a simple way of obtaining reasonable rough estimates of the bound electron level energies using a simple hydrogenic–continuum model. As with the discretized screened hydrogenic model [6], the energy levels obtained are essentially the ground states of the Bohr Hamiltonian,

$$H_n = \frac{p^2}{2m} - V + \frac{\hbar^2 n^2}{2mr^2} \tag{38}$$

for $n \geq 1$. The electrostatic potential V is constructed for a series of concentric shells continuously populated according to an assumed density–of–states $g(n)$, up to a maximum $n = N$ such that $\int_0^N g(n)dn = Z-Z^*$. The energy levels for integral values of n are then extracted, in accordance with the virial theorem, as $E_n = -\frac{1}{2}V(r_n)$ where $r_n \equiv 1/u_n$ is the classical orbit radius ($n>1$) or s–orbital uncertainty radius ($n=1$) as given by

$$u_n = \frac{1}{n^2 a}\frac{\partial V}{\partial u}\Big|_{u=u_n} \tag{39}$$

with $u \equiv 1/r$. This procedure yields the energy levels according to

$$E_n = -\frac{\alpha\hbar c}{2}\left[Z_n u_n - \int_n^N u_\nu g(\nu)\mathrm{d}\nu \right] \tag{40}$$

for $u \leftrightarrow n$ being continuous, differentiable and one–to–one in $n \geq 1$, $u > 0$, and where

$$Z_n = Z + 1 - \int_0^n g(n)dn, \quad N \geq n > 1; \qquad Z_n = Z \text{ or } Z - \frac{1}{2}, \quad n = 1 \tag{41a,b}$$

is the charge inside the orbital n. The use of $Z+1$ instead of Z in (41a) corrects for the self–energy of the electron in the orbit n. With $g(n) = 4n$, the simplest reasonable choice, the model yields the spectrum

$$E_n = -E_R\left[\left[\frac{Z+1}{n}\right]^2 - 4(1+Z)\left[1 + \tfrac{1}{2}\ln\left[\frac{Z-Z^*}{2n^2}\right]\right] + 2(Z-Z^*)\right], \quad 1 \leq n \leq \left[\frac{Z-Z^*}{2}\right]^{\frac{1}{2}} \tag{42a}$$

$$= -E_R\left[\frac{Z^*+1}{n}\right]^2, \qquad n \geq \left[\frac{Z-Z^*}{2}\right]^{\frac{1}{2}} \tag{42b}$$

$$= -E_R\left[(Z-1)^2(Z-Z^*-1) + Z^2(2-Z+Z^*)\right], \qquad n = 1,\ 1 \leq Z - Z^* \leq 2 \tag{42c}$$

$$= -Z^2 E_R, \qquad n = 1,\ (Z-Z^*) \leq 1 \tag{42d}$$

where E_R is the Rydberg energy. An *ad hoc* generalisation of the above parameterisation permits some fine tuning through the introduction of an adjustable parameter α which can be used to fit the spectrum to available data. In place of (42a), the formula actually used is

$$E_n = -E_R\left[\left[\frac{Z+1}{n}\right]^2 - 4(1+Z)\left\{1 + \ln\left[\alpha + \left[\frac{Z-Z^*}{2}\right]^{\frac{1}{2}}\right] - \ln[\alpha + n]\right\} + 2(Z-Z^*)\right] \tag{43}$$

in which α is parameterised in terms of $Z-Z^*$ so as to fit the K–shell ionization energies of the neutral atoms across the periodic table. Typically (ie, for $Z-Z^* \lesssim 70$) $-\frac{1}{2} < \alpha < 1$. This model can also be used to construct (piecewise) analytical atomic potentials which, unlike Thomas–Fermi, can be calculated without recourse to numerical integration.

The parameterised form of $\alpha(x = Z-Z^*)$ is as follows:

$$\alpha(x) = \alpha^0(x) + \alpha^1(x)$$

where

$$\alpha^0(x) = \begin{cases} 0 & x \leq 1 \\ -0.069685 & 1 \leq x \leq 2 \\ 0.069685(x-3) + 0.80176(x-2) & 2 \leq x \leq 3 \\ \dfrac{(x+35.2)(x-15)(x-56.7)}{74.19(x+1.7)(91.05-x)} & 3 \leq x \end{cases}$$

and

$$\alpha^1(x) = 0.1426\ x^{-\frac{1}{2}}\ \sin[\tfrac{1}{2}\pi(\sqrt{(4x+165)} - 11)] \qquad 4 < x < 41$$

$$= 0 \qquad x \leq 4;\ x \geq 41$$

Finally, the ionization energies provided to the average-atom model need to be further adjusted to account for continuum lowering in the plasma. ie,

$$\varepsilon_n = -E_n + \Delta V_{c1} \qquad (44)$$

This is also the opportunity to correct for any degeneracy in the continuum.

4 - NUMERICAL CALCULATIONS

Numerical calculations have been carried out with Supercalc™4 spreadsheets running on an 80386/387 personal computer. These calculations are performed in two stages. First the plasma model is self-consistently solved and the plasma properties necessary to determine the stopping power calculated. The second stage integrates the stopping-power equation (1) over its range of validity to determine the particle range and the energy deposition rate, dE/dx vs x. (The plasma model also yields the specific heat, so that, knowing the ion beam flux gives local rate of temperature increase.) Inner-shell corrections are applied where necessary.

Two (arbitrary) plasmas were modelled, namely aluminium at T=100eV, and lead at T=300eV, both at normal density. The computed values of $\bar{I}$ are respectively 102eV and 459eV. The plasma coupling parameters work out respectively at Γ=1.65 and Γ=2.4 compared with the OCP values of 7.35 and 53.6 respectively. The values of the ratio, D_e/R, of the electron Debye length to the ion-sphere radius are 0.663 for the aluminium, and 0.545 for the lead example, showing that there is a significant degree of free electron polarization. The resulting values of $Z_2{}^*/Z^*$ are 0.933 and 0.885 respectively. Under these conditions, the total continuum lowering in the aluminium is found to be about 140 eV, of which 16 eV is attributed to continuum fluctuations, while for the lead, it is found to be about 680 eV with a fluctuation component of 60eV. Application of the Stewart-Pyatt formula from [6] yields, for the same values of Z^*, 116 and 590 eV respectively. These effects lead to increased ionization (increased Z^*) within the plasma.

The results of some model calculations are shown in the figures. In interpreting these figures the following explanatory notes may be helpful: Dashed lines denote the results of using equation (1) without inner-shell corrections, where these show a difference. Excitation functions are given in arbitrary units. The stopping power $S(E)$ is $(1/\rho)|dE/dx|$ in MeVcm^2/g units. The range is the total distance travelled by the ion (proton) before coming approximately to rest. The mean free path is $\bar{I}/|dE/dx|$ with any inner-shell correction to $\bar{I}$ is applied by computing the average of $\ln(\omega)$ over the interval $0 < \omega < q$. In the captions, "ion" and "proton" are synonymous. It is hoped that the figures are otherwise self-explanatory.

The excitation functions show clearly the plasma collective "resonance" (at 31 eV in the aluminium and 59 eV in the lead) and also a series of edge features (counting from the right these are the K and L features in the aluminium; and the K, L, M, N, O features in lead). The peak of the plasma resonance is found, in these examples, to be significantly above the plasma frequency, ω_e which is 26.6 eV and 45.7 eV respectively.

5 - CONCLUSIONS

A simple yet powerful plasma model has been described and applied to some examples. The calculations show that in high-Z plasmas of moderate to high density, the corrections that one needs to apply to the ion-ion interaction to account for electron polarisation and screening are large. This is indicative of failure of the OCP. model. The model described here, while plausible, is clearly capable of further refinement where the necessary extra computing power is available. This model, as described, was developed principally for rapid calculations over wide parameter ranges and for assessing the importance of various physical processes, rather than for accurate calculations in narrow parameter ranges.

Calculations show that the simple relativistic stopping power formula (1) is useful for determining where a fast heavy ion deposits *most* of its energy in hot plasma, and for estimating the ion's range in that plasma. A virtue of (1) is its simplicity and the ease with which it can be incorporated into a calculation of the plasma hydrodynamics. The necessary tables of $\bar{I}(\rho,T)$ are easily provided. It is found that applying a simple "inner-shell correction" to (1) is advantageous and results in a more reasonable description near the end of the ion's range. However knowledge is then required of the excitation spectrum.

The representation of the plasma properties, in the stopping power treatment, through the dielectric function enables a description of both the collective plasma processes due to free electrons, and ionization processes involving bound electrons, in a convincing and unified way.

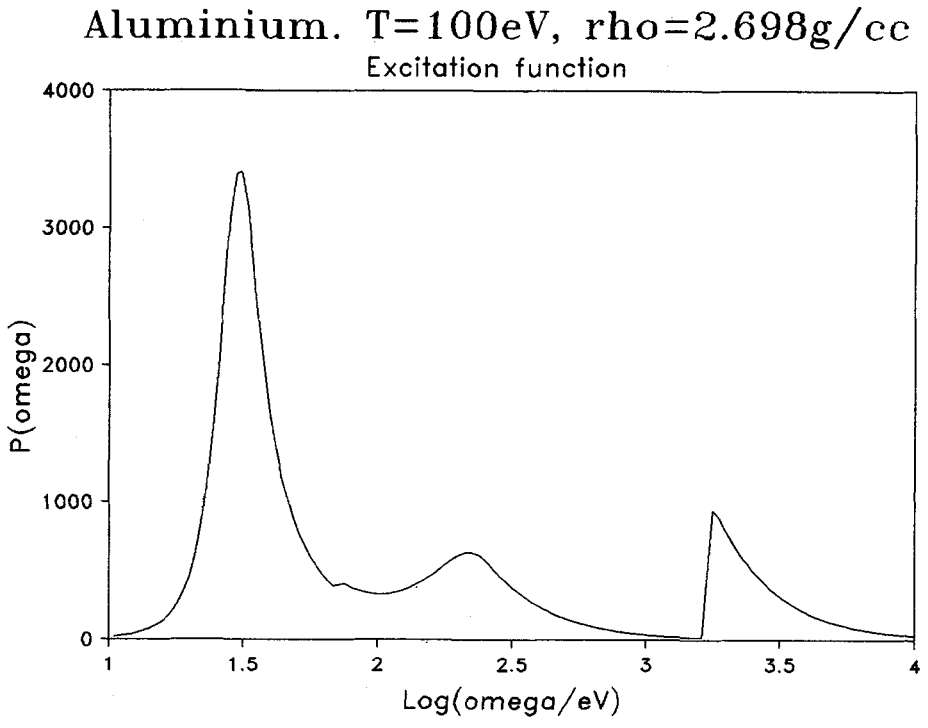
Aluminium. T=100eV, rho=2.698g/cc
Excitation function
4000
3000
2000
1000
0
P(omega)
1
1.5
2
2.5
3
3.5
4
Log(omega/eV)

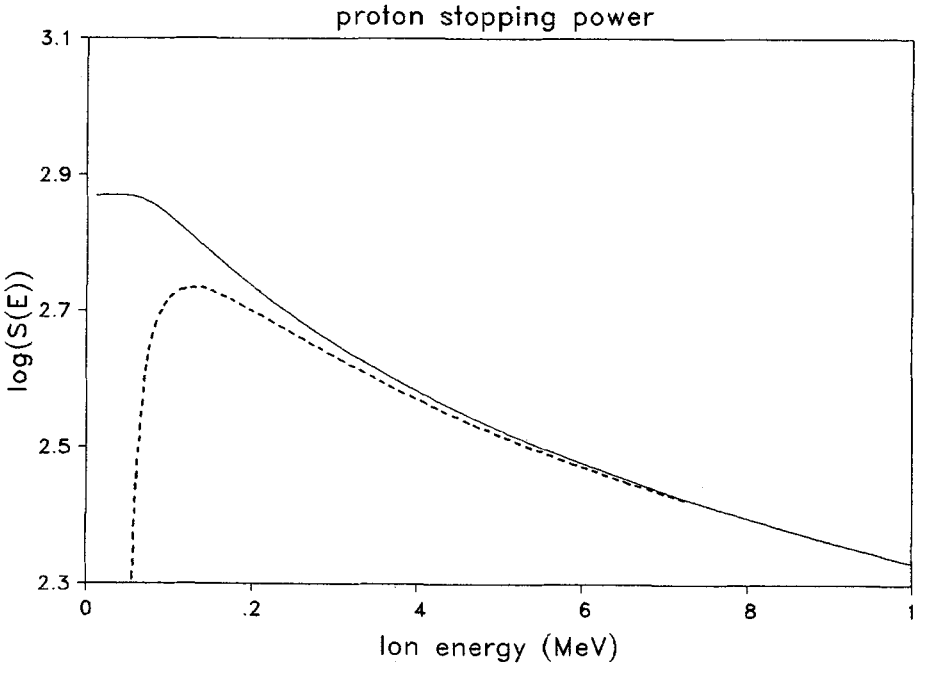
Aluminium. T=100eV, rho=2.698g/cc
proton stopping power
3.1
2.9
2.7
2.5
2.3
log(S(E))
0
.2
4
6
8
1
Ion energy (MeV)

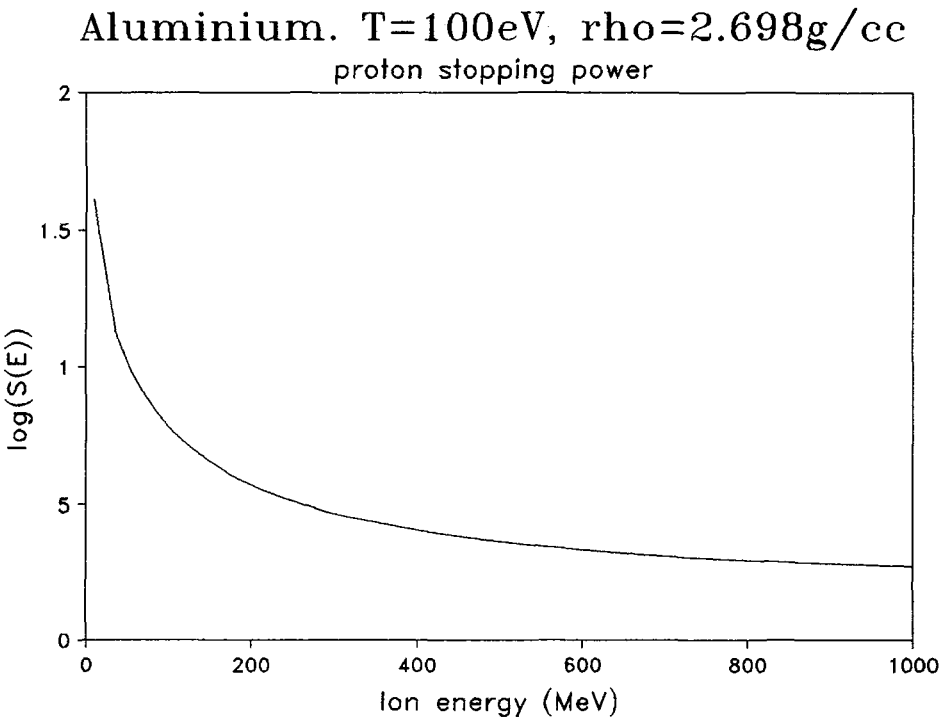
Aluminium. T=100eV, rho=2.698g/cc
proton stopping power
log(S(E))
2
1.5
1
5
0
0
200
400
600
800
1000
Ion energy (MeV)

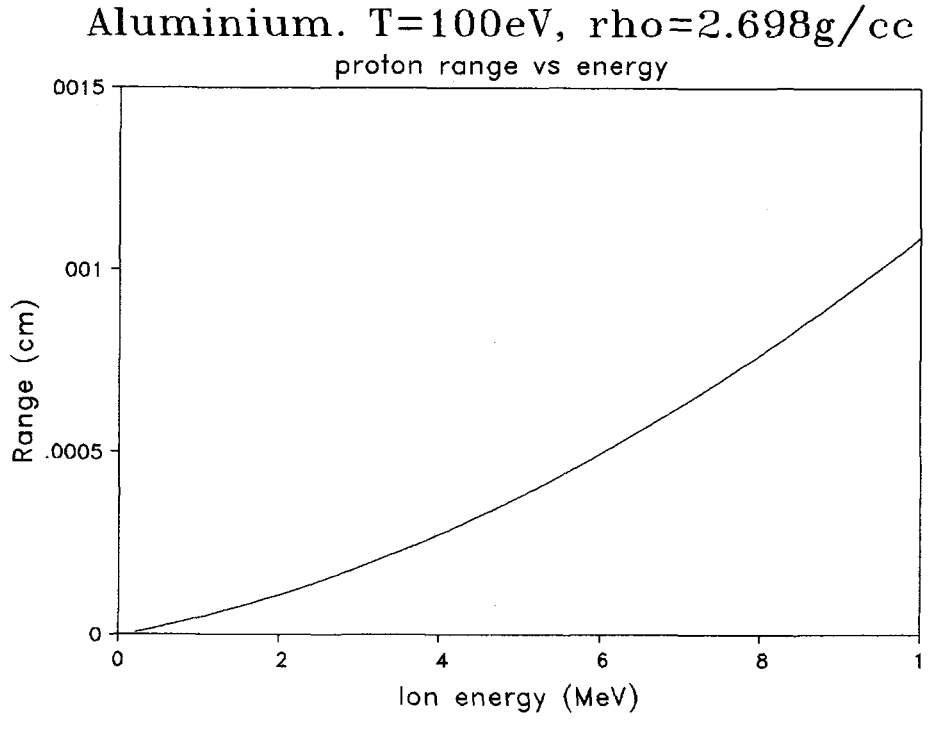
Aluminium. T=100eV, rho=2.698g/cc
proton range vs energy
Range (cm)
0015
001
.0005
0
0
2
4
6
8
1
Ion energy (MeV)

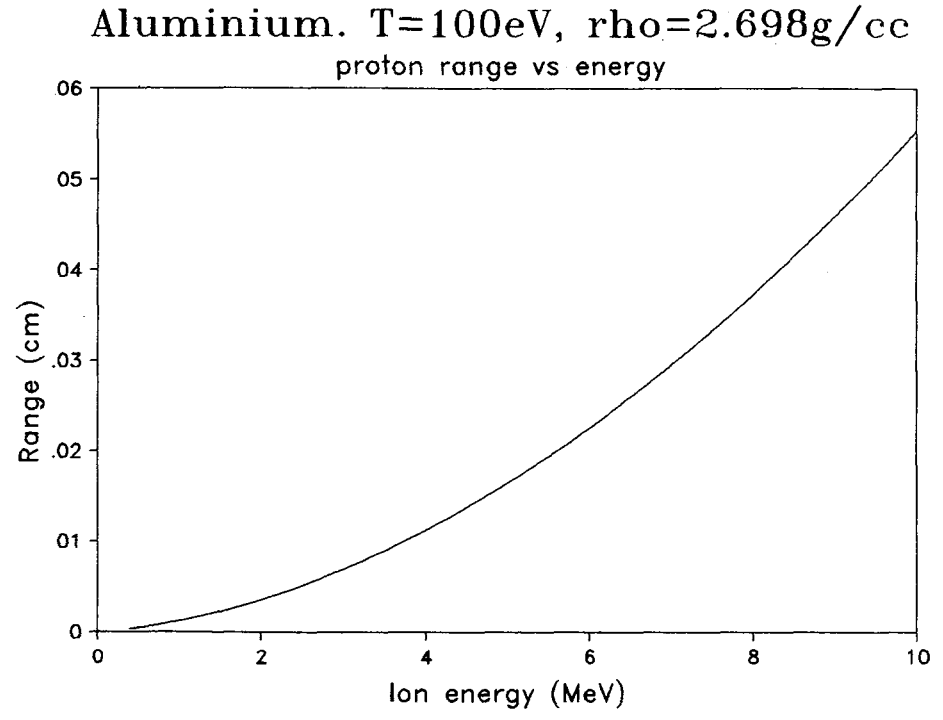
Aluminium. T=100eV, rho=2.698g/cc
proton range vs energy
Range (cm)
.06
05
04
.03
.02
01
0
0
2
4
6
8
10
Ion energy (MeV)

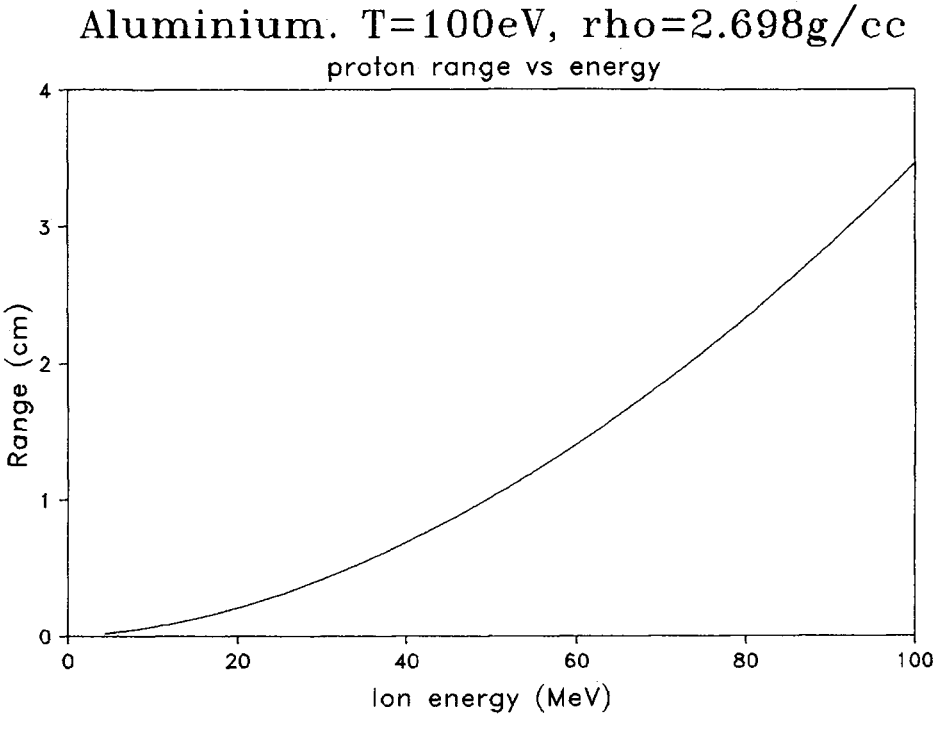
Aluminium. T=100eV, rho=2.698g/cc
proton range vs energy
Range (cm)
4
3
2
1
0
0
20
40
60
80
100
Ion energy (MeV)

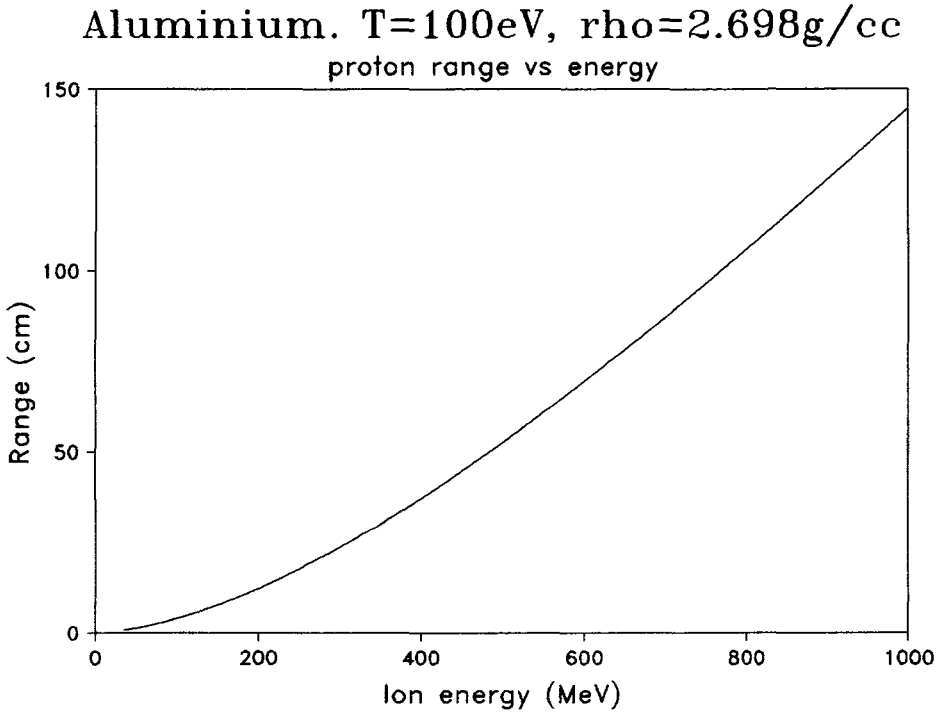
Aluminium. T=100eV, rho=2.698g/cc
proton range vs energy
150
100
50
0
Range (cm)
0
200
400
600
800
1000
Ion energy (MeV)

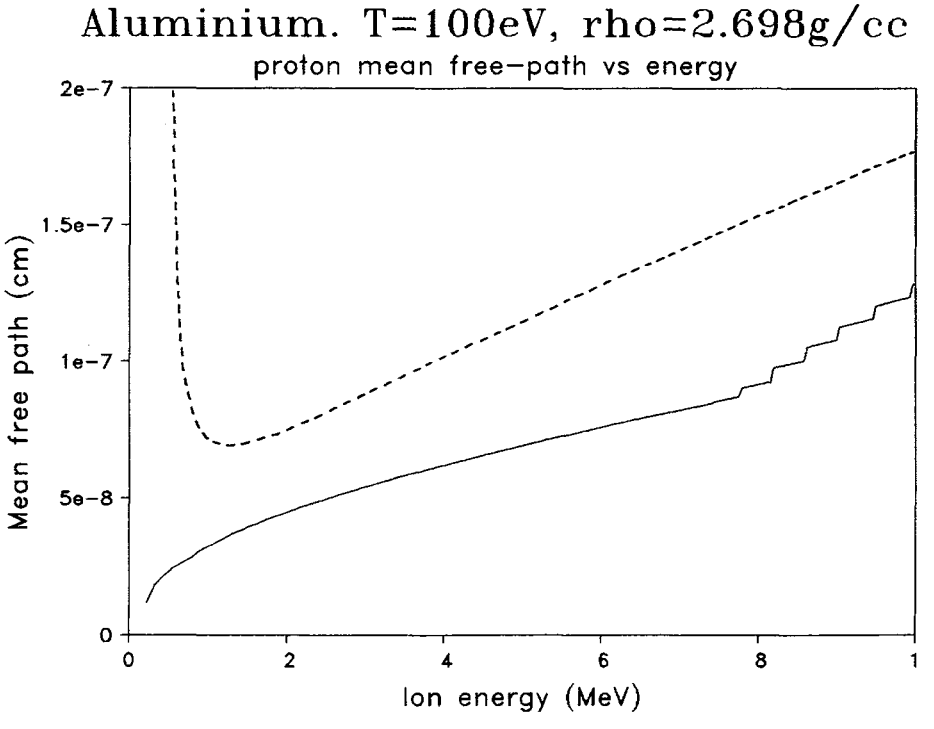
Aluminium. T=100eV, rho=2.698g/cc
proton mean free-path vs energy
2e-7
1.5e-7
1e-7
5e-8
0
Mean free path (cm)
0
2
4
6
8
1
Ion energy (MeV)

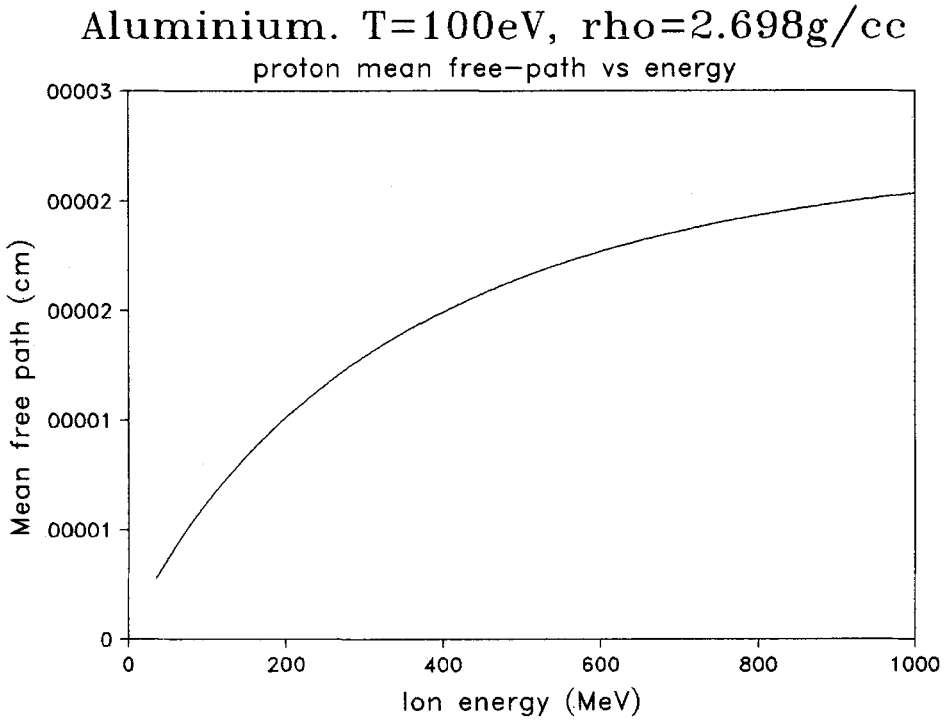
Aluminium. T=100eV, rho=2.698g/cc
proton mean free-path vs energy
Mean free path (cm)
00003
00002
00002
00001
00001
0
0
200
400
600
800
1000
Ion energy (MeV)

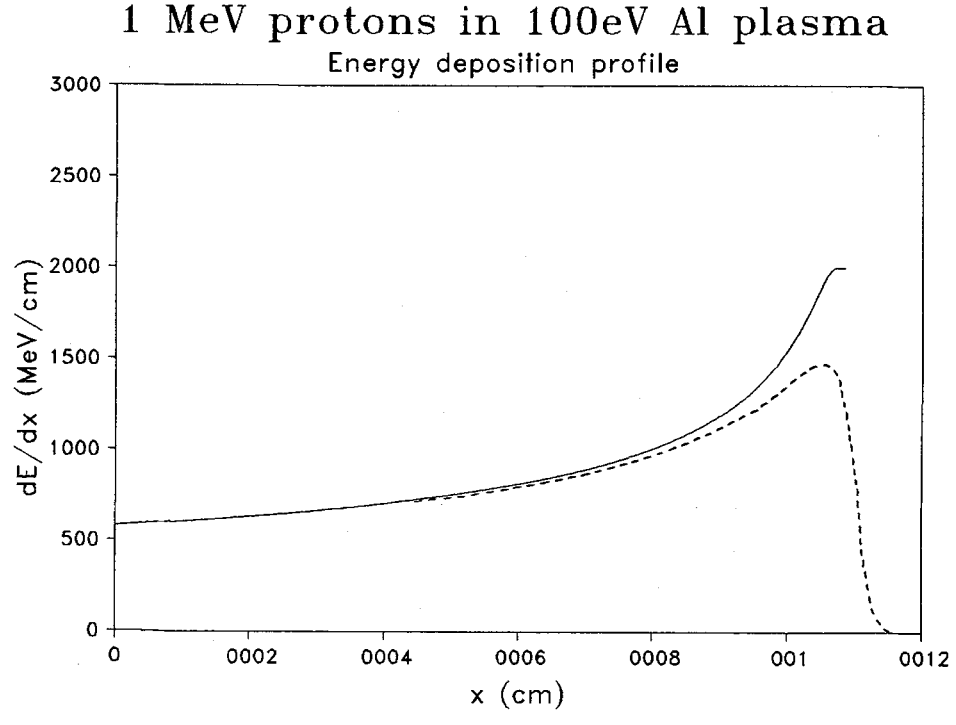
1 MeV protons in 100eV Al plasma
Energy deposition profile
dE/dx (MeV/cm)
3000
2500
2000
1500
1000
500
0
0
0002
0004
0006
0008
001
0012
x (cm)

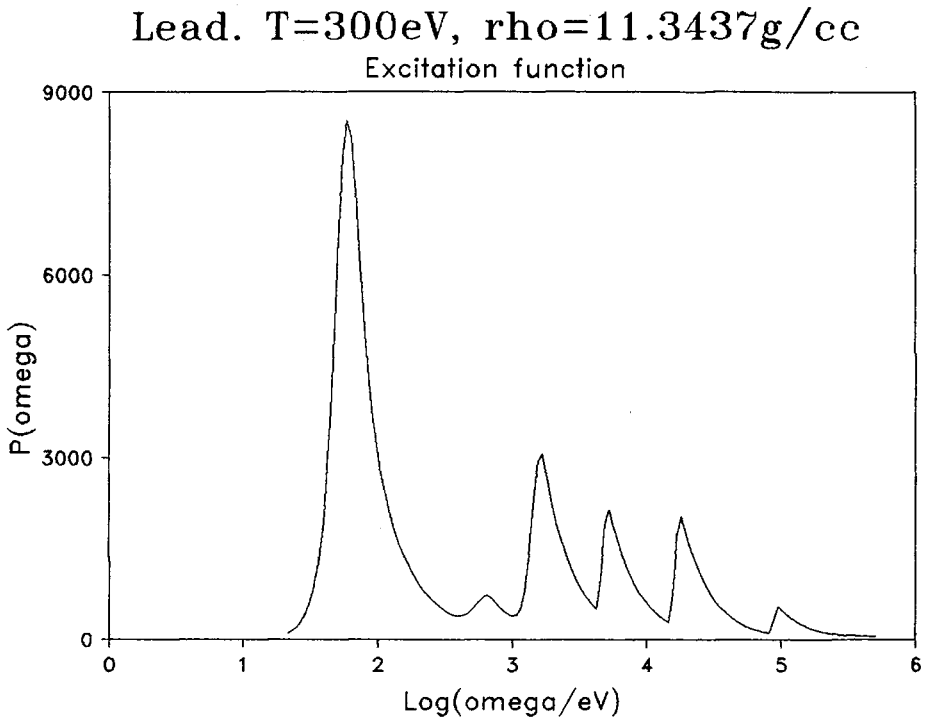
Lead. T=300eV, rho=11.3437g/cc
Excitation function
9000
6000
3000
0
P(omega)
0
1
2
3
4
5
6
Log(omega/eV)

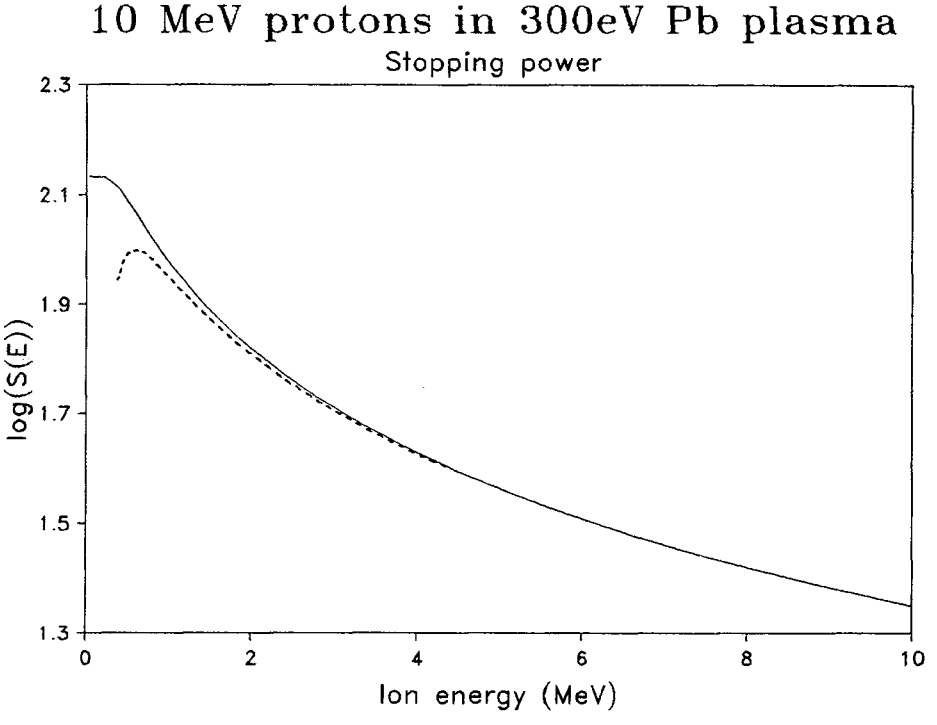
10 MeV protons in 300eV Pb plasma
Stopping power
2.3
2.1
1.9
1.7
1.5
1.3
log(S(E))
0
2
4
6
8
10
Ion energy (MeV)

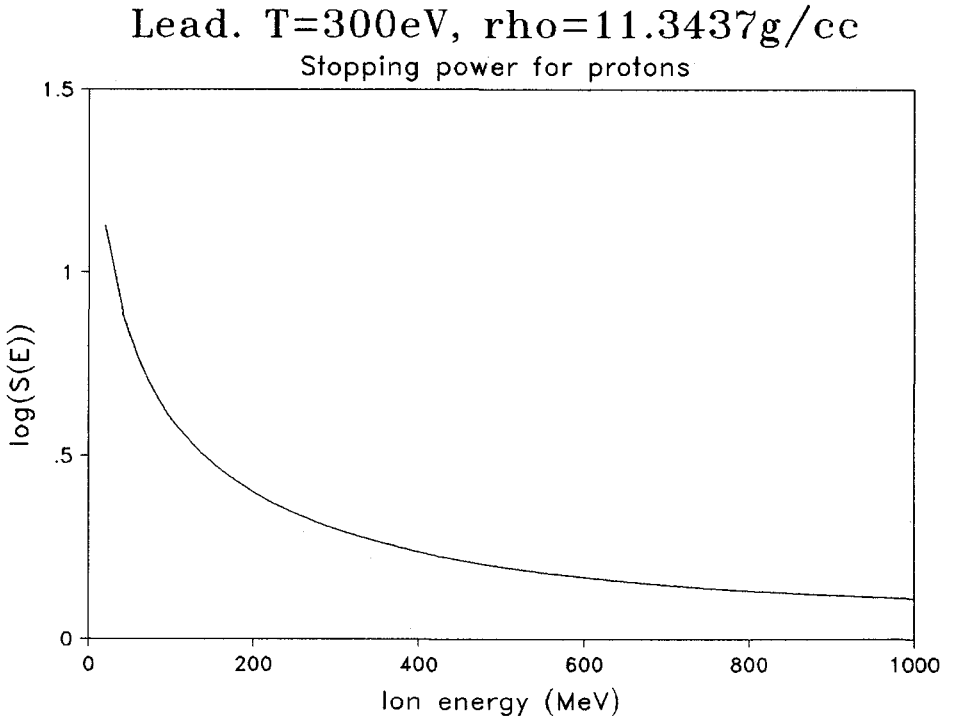
Lead. T=300eV, rho=11.3437g/cc
Stopping power for protons
log(S(E))
1.5
1
.5
0
0
200
400
600
800
1000
Ion energy (MeV)

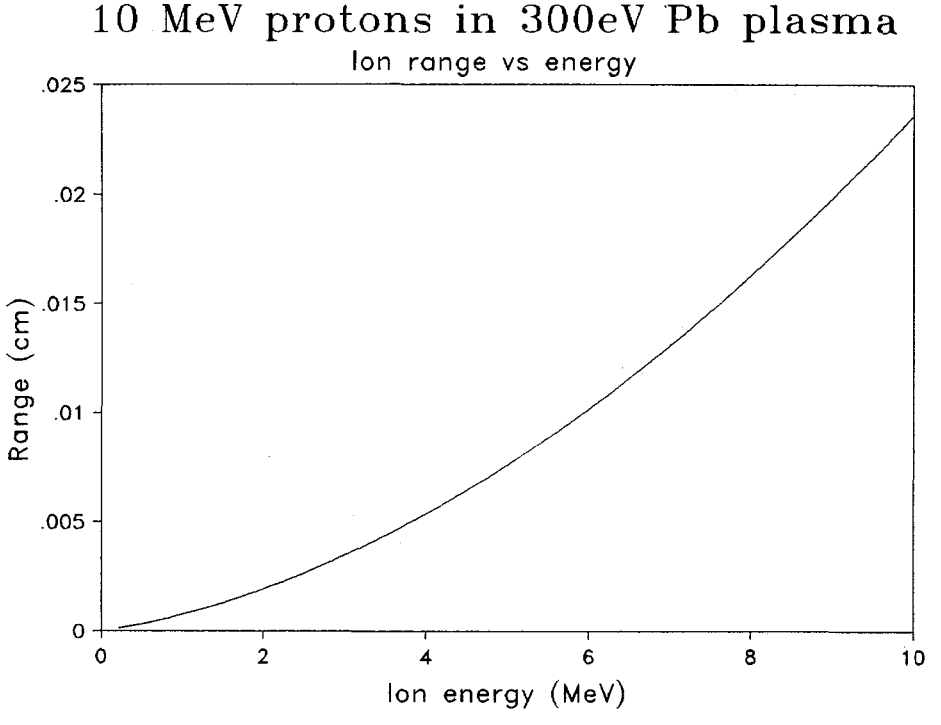
10 MeV protons in 300eV Pb plasma
Ion range vs energy
Range (cm)
.025
.02
.015
.01
.005
0
0
2
4
6
8
10
Ion energy (MeV)

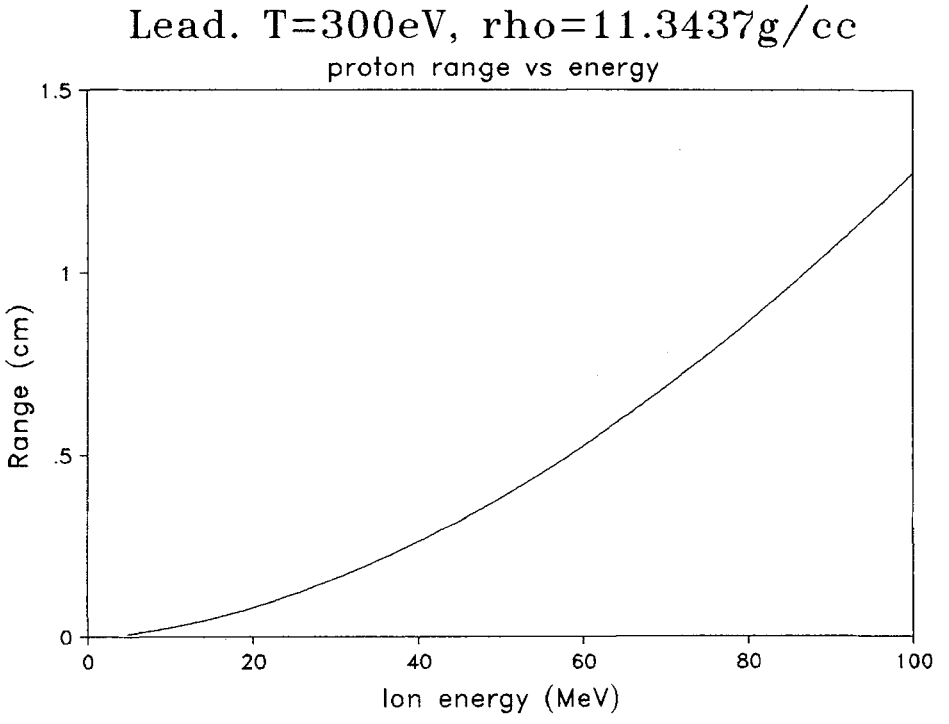
Lead. T=300eV, rho=11.3437g/cc
proton range vs energy
Range (cm)
1.5
1
.5
0
0
20
40
60
80
100
Ion energy (MeV)

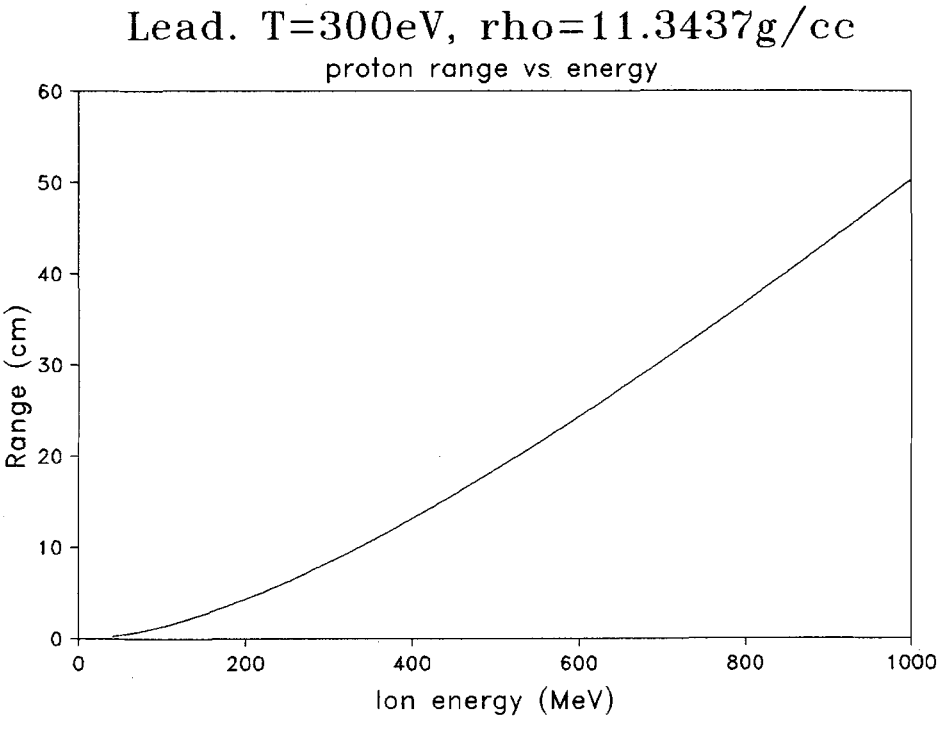
Lead. T=300eV, rho=11.3437g/cc
proton range vs energy
Range (cm)
60
50
40
30
20
10
0
0
200
400
600
800
1000
Ion energy (MeV)

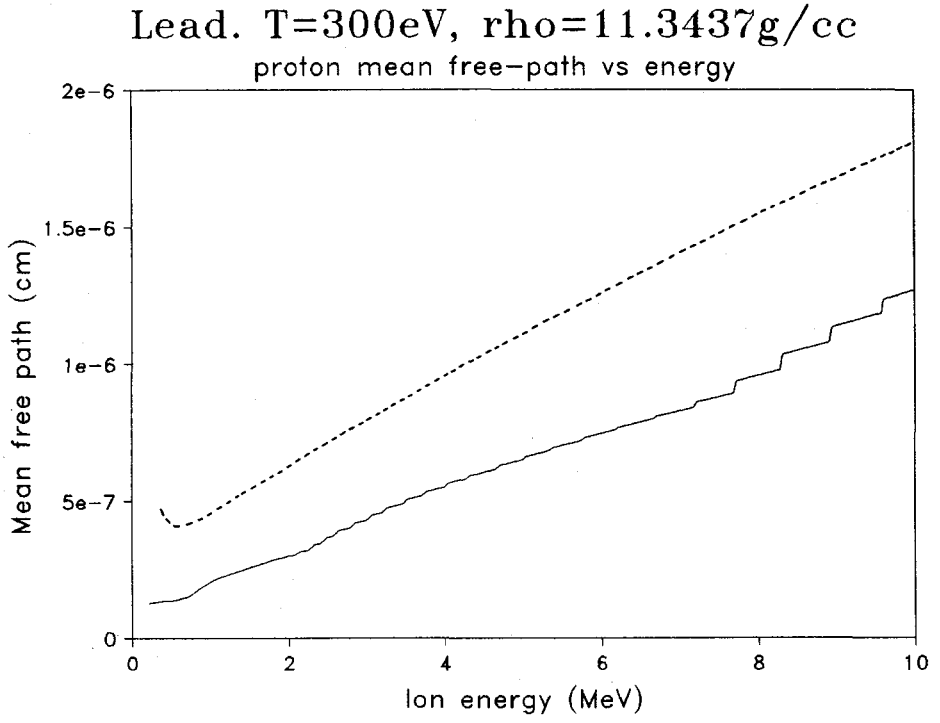
Lead. T=300eV, rho=11.3437g/cc
proton mean free-path vs energy
Mean free path (cm)
2e-6
1.5e-6
1e-6
5e-7
0
0
2
4
6
8
10
Ion energy (MeV)

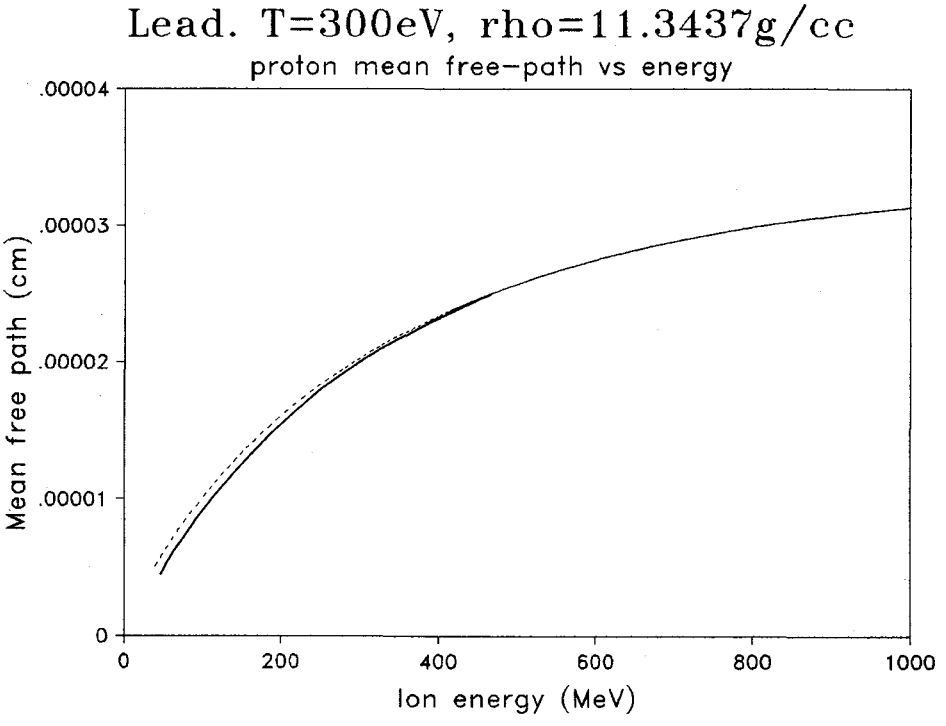
Lead. T=300eV, rho=11.3437g/cc
proton mean free-path vs energy
Mean free path (cm)
.00004
.00003
.00002
.00001
0
0
200
400
600
800
1000
Ion energy (MeV)

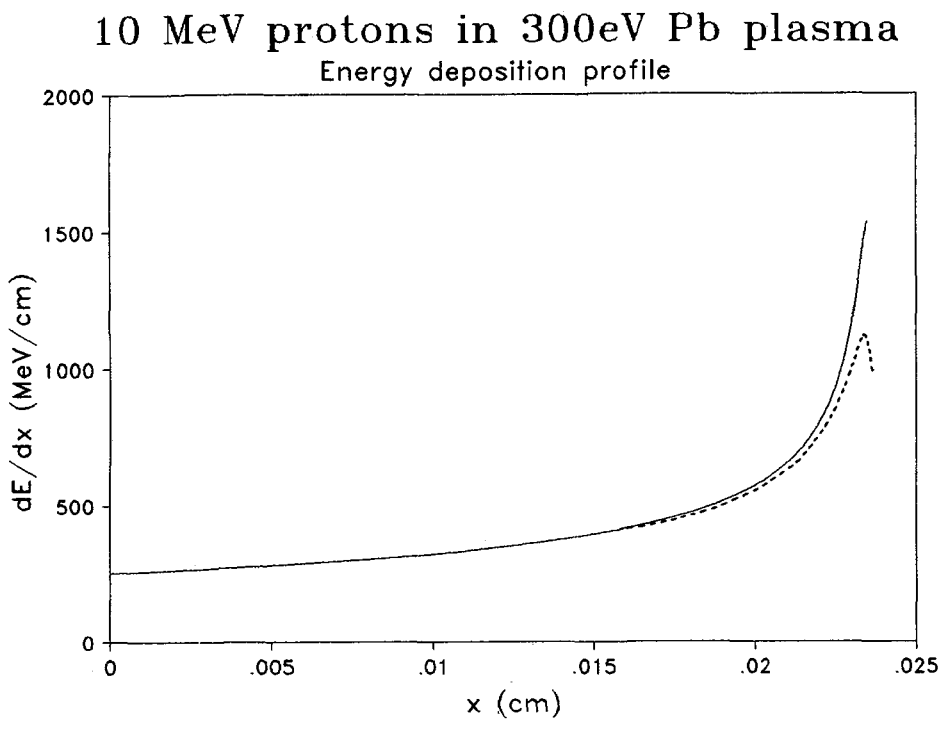

REFERENCES

[1] Landau, L.D., Lifshitz, E.M. and Pitaevskii, L.P., *Electrodynamics of Continuous Media* (2nd edition, Pergamon Press, 1984) ch.XIV.
[2] Crowley, B.J.B. in *Proceedings of the Second International Workshop on Atomic Physics for Ion Fusion*, eds. T.D.Beynon and J.H.Aram (Rutherford-Appleton Laboratory, 1984) vol.2, p.359
[3] Spitzer, L., *Physics of Fully Ionized Gases* (Interscience, N.Y., 1956)
[4] Karzas, W.J. and Latter, R., *Astrophys.J.*Supplement No.55, vol.6 (1961) 167-212.
[5] Mott, N. and Jones, H., *Theory of the Properties of Metals and Alloys* (OUP, 1936).
[6] More, R.M., *Atomic Physics in Inertial Confinement Fusion,* UCRL-84991 (1981) part 1.
[7] More, R.M., *Atomic Physics in Inertial Confinement Fusion,* UCRL-84991 (1981) part 2.
[8] Skupsky, S., *Phys.Rev.*A, 16 (1977) 727-731
[9] Landau, L.D., Lifshitz, E.M. and Pitaevskii, L.P., *Physical Kinetics* (Pergamon Press, 1981) ch.IV.
[10] Bethe, H.A. and Salpeter, E.E., *Quantum Mechanics of One- and Two-Electron Atoms* (Springer-Verlag, 1957) section 76.
[11] Zel'dovich, Ya., and Raizer, Yu., *Physics of Shock Waves and High Temperature Hydrodynamic Phenomena* (Academic Press, 1966).
[12] Brush, S., Sahlin, H. and Teller, E., *J.Chem.Phys.* 45 (1966) 2102.
[13] DeWitt, H., *Phys.Rev.*A 14 (1976) 1290.
[14] Latter, R., *Phys.Rev.* 99 (1955) 1854-1870.
[15] Bradley, D.K., Kilkenny, J., Rose, S.J. and Hares, J.D., *Phys.Rev.Letts.* 59 (1987) 2995-2998.
[16] Lindhard, J., Nielsen, V. and Scharff, M., *Det Kong Danske Vidensk Selsk* 36 (1968) 10.
[17] Stewart, J. and Pyatt, K., *Astrophys.J.* 144 (1966) 1203.